Single-pulse nuclear spin echo in magnets

I. G. Kiliptari
Physics Department, Tbilisi State University, Tbilisi 380028, Republic of Georgia

V. I. Tsifrinovich
Department of Applied Mathematics and Physics, Polytechnic University, 6 Metrotech Center, Brooklyn, New York 11201

(Received 4 June 1997; revised manuscript received 16 January 1998)

A detailed experimental investigation of a wide variety of ferromagnetic materials has been undertaken in order to study the properties of the single-pulse echo arising after the application of a solitary resonance rf pulse to an inhomogeneously broadened nuclear spin system. The investigation is based on a comparative analysis of the single- and two-pulse echo. By means of a dc magnetic-field pulse applied coincident with the exciting rf pulse, the crucial role of edge distortions of the latter in the formation of the single-pulse echo has been demonstrated. The experimental data are compared with computer calculations performed for a system of weakly interacting spins. The principal result of these calculations is that strictly rectangular pulses are unable to produce a single-pulse echo. However, the solution of the Bloch equations for a pulse with phase shifted edges results in the formation of a single-pulse echo. The calculated echo profiles are sensitively dependent upon the pulse distortion parameters, and show reasonable agreement with the corresponding experimental data. [S0163-1829(98)10917-7]

I. INTRODUCTION

In recent years, pulsed transient methods have been widely used to study coherent processes in various kinds of inhomogeneous systems. In these methods a sample is subjected to a coherent sequence of excitation pulses, while the detection of the response is usually performed in the absence of the exciting stimuli, when the system freely evolves.

At the present time, echolike pulse responses of magnetic, electric, or acoustic origin have been observed in a wide range of physical systems. Depending on the echo formation dynamics, all these systems can be separated into two groups. In systems of weakly interacting particles the echo processes are described by the Bloch equations of motion,[1,2] while in strongly interacting systems they are commonly associated with anharmonic-oscillator interactions.[3]

Generally two or more stimulating pulses are required to give rise to echo phenomena. In practice, however, an echo can also be generated in the case of single-pulse excitation. Bloom[4] was first to observe the single-pulse echo (SPE) phenomenon in an inhomogeneously broadened proton NMR system and attributed it to the coherence of nonresonant spin packets. Later the SPE has been found to occur in experiments on electron[5] and photon[6] echoes, as well as in piezoelectric crystalline[7] and powdered samples.[8] Similar observations have been made on ^{59}Co nuclei in ferromagnetic cobalt[9] and also on ^{55}Mn nuclei in antiferromagnetic $MnCO_3$ and $CsMnF_3$.[10] These results have stimulated extensive discussions in the literature regarding the origin of SPE.[7–17]

It has been pointed out repeatedly that despite the substantial dissimilarities of the systems producing SPE signals they are characterized by a number of common properties. In particular, it has been observed that SPE appears at a time approximately equal to the pulse length τ_1 after its termination, and under conditions where the inhomogeneous broadening is greater than the frequency width of the exciting pulse. The intensity of SPE is also much smaller than the intensity of two-pulse echo (TPE), while its phase in the long-pulse limit is opposite to that of a free induction decay (FID).[7–12] Thus it seems appropriate to consider the problem of SPE on more general grounds, regardless of the physical properties of a particular system under consideration. We therefore assume that the formation of SPE is controlled by pulse distortions, which necessarily arise in the course of exciting the systems.

For example, in the radio frequency (rf) region the most common distortions of a rectangular pulse are finite rise and fall times, peak voltage sag and oscillations, which cause phase modulation of the rf pulse carrier frequency.[18–21] Distortions of this kind may originate in different pieces of the electronic apparatus, such as cascade amplifiers and pulse generators, or may be due to the lack of necessary matching in the rf oscillator driving circuitry.

The major difficulty encountered in analyzing the SPE phenomenon is that the signal of interest is commonly obscured by the simultaneous presence of a nonmonotonic FID produced immediately after a single exciting pulse. Hence the problem reduces to one of separating the SPE from the oscillatory FID. This cannot be generally done unambiguously.[22,23] From this point of view, the most favorable sample materials are magnetically ordered substances, since the inhomogeneity of the rf enhancement factor η in these samples is expected to smear out the oscillations in the FID making it possible to perform a comprehensive study of SPE. Thus with regard to the SPE phenomenon the nuclear spin system in ferromagnets may serve as a simple test model.

In the present paper, we report an investigation of the SPE phenomenon, based on complete experimental and theoretical studies in a wide range of ferromagnets. The structure and the main results of the paper are as follows. Section II presents a comparison of results from SPE and TPE experi-

TABLE I. Values for various parameters of the primary group of magnets at $T=77$ K.

Sample	Crystal structure	Nucleus	Nucleus spin	Frequency ν_0 (MHz)	I_m^S/I_m^T (%)	T_2, T_2^S (μs)	$\overline{\eta_0}\times 10^3$
$Li_{0.5}Fe_{2.5}O_4$	Ferrite-spinel class	^{57}Fe	$\frac{1}{2}$	74.0	14.1	4000[a]	220[a]
						2000[b]	200[b]
Co_2MnSi	Cubic of Cu_2 MnAl type	^{59}Co	$\frac{7}{2}$	145.2	13.7	38[a]	8.0[a]
						23[b]	7.5[b]
		^{55}Mn	$\frac{5}{2}$	253.1	11.6	80[a]	5.6[a]
						58[b]	5.2[b]
$Mn_{0.51}Sb_{0.49}$	hcp of NiAs type	^{123}Sb	$\frac{7}{2}$	208.0	13.5	170[a]	6.8[a]
						135[b]	6.7[b]
		^{55}Mn	$\frac{5}{2}$	256.5	12.0	60[a]	4.0[a]
						42[b]	4.3[b]
Co	fcc	^{59}Co	$\frac{7}{2}$	217.2	12.3	30[a]	1.5[a]
						20[b]	1.8[b]
Co	hcp	^{59}Co	$\frac{7}{2}$	219.0[c]	12.7	65[a]	0.8[a]
						42[b]	0.8[b]
				227.0[c]	11.1	40[a]	1.0[a]
						29[b]	1.2[b]
NiMnSb	orthorhombic of MgAgAs type	^{55}Mn	$\frac{5}{2}$	298.4	9.8	95[a]	0.9[a]
						76[b]	0.8[b]
NiMnSi	orthorhombic of MgAgAs type	^{55}Mn	$\frac{5}{2}$	320.5	9.2	60[a]	1.1[a]
						50[b]	1.0[b]

[a]Values of parameters obtained by the two-pulse echo technique.

[b]Values of parameters obtained by the single-pulse echo technique.

[c]The existence of two discernible peaks at 219.0 and 227.0 MHz in hcp Co is commonly attributed to the wall edge and wall center resonances, respectively (Ref. 17). A somewhat overestimated value of $\overline{\eta_0}$ for the former resonance is probably due to the admixture of fcc phase having relatively high values of enhancements. The difference in all the quoted values for powdered samples and thin ferromagnetic films of hcp Co does not generally exceed 5%.

ments. Special emphasis is placed upon direct experimental verification of the dominant role of pulse distortions in the SPE formation process. In Sec. III we derive the general expressions which describe explicitly the induced nuclear magnetization following a single pulse with arbitrary phase distortions at its edges. We also report the results of numerical calculations of the NMR signals obtained under different excitation conditions. Finally, in Sec. IV a careful analysis of the single echo formation mechanisms is carried out, and general requirements for the production of SPE are discussed in detail.

II. EXPERIMENTAL

A. Sample characterization

Experiments were carried out on various ferromagnetic bulk materials and thin films, with different crystal structure and magnetic properties. Structure, nuclear spin, and some other characteristics of the primary group of magnetic materials are summarized in Table I. In addition, measurements were made on a series of magnets based on several of the tabulated materials, including cobalt fcc alloys with all of the $3d$ transition metals (Ti, V, Cr, Mn, Fe, Ni, and Cu) having maximum impurity content up to 8 at. %, $Mn_{1-x}Sb_x$ alloys in the concentration range $0.43\leqslant x\leqslant 0.49$, and diamagnetically diluted ferrites of $Li_{0.5}Fe_{2.5-x}Zn_xO_4$ ($0\leqslant x\leqslant 0.25$). On the whole about 40 different samples have been synthesized and examined.

Metallic ferromagnetic alloys and compounds were prepared by melting together the appropriate amounts of bulk or powdered constituents in an induction vacuum or a direct-arc furnace. The starting materials were of the following purity: 99.999% Sb, 99.995% Mn, and 99.98% all the other elements. All samples were polycrystalline multidomain materials with a high abundance of magnetically active nuclei, that is, of about 50% for ^{123}Sb and 100% for ^{59}Co and ^{55}Mn. Metallic ingots were sealed in evacuated quartz tubes, annealed for 300–700 h in the temperature range 700–1000 °C and then filed to powder form with the particle size less than 50 μm. Preparation technique, temperature, and the annealing treatment of both bulk and powdered samples were modified, depending on the particular system under consideration.

Circular disks of dielectric lithium ferrite and its solid solutions, of 12–15 cm in diameter and 5–8 g in weight, were produced by means of a conventional ceramic preparation technique using an enriched (96.8 at. % ^{57}Fe) iron isotope.

Cobalt monolayer thin ferromagnetic films with thickness from 800 to 1200 Å were grown by ion-beam vacuum sput-

tering on glass substrates in an in-plane magnetic field of 100 Oe, and contained about 70% of hcp and 30% of fcc phase. It is worth noting here that the most intense NMR spin-echo signals were found to occur for the rf field h, applied perpendicular to the easy axis of magnetization in the plane of a film, while in the direction of this axis no echoes could be detected. This implies that the echo signals in these films arise from domain rather than from domain wall.[24] Unlike ferromagnetic films, all the powdered and bulk samples in zero external field exhibit NMR signals that originate predominantly from the domain-wall nuclei.[17,25]

B. Experimental apparatus

A standard phase-incoherent spin-echo spectrometer[25,26] was employed in the present measurements of the NMR signals appearing after a single- or a two-pulse sequence at both 77 and 293 K. The receiver of such a spectrometer operates through amplitude detection only, i.e., the physical quantity observed is the absolute value of the nuclear macroscopic magnetization in the equatorial plane and not its phase. All the experiments were performed in the frequency range 40–400 MHz, the pulse repetition time being nearly tenfold longer than the longitudinal relaxation time of the sample. In the frequency range 40–220 Mhz a standard self-excitation rf oscillator has been used. The frequency of the oscillator could be gradually returned by using a number of circuits with different inductance coils and adjustable capacitors. In the frequency range 200–400 Mhz the excitation was carried out with the aid of a commercial manufactured oscillator based on the two-wire Lekher-type line including two coils with different number of turns. For pulse lengths ranging between 0.1 and 50 μs a maximum rf field produced at the sample was estimated to be about 3.0 Oe, while the rise and fall times of sufficiently long pulses ($\tau_1 \gtrsim 5\ \mu$s) were no more than 0.15 μs. At 1.0–1.5 W input powers the recovery time of the spectrometer characterizing the transient loss of its sensitivity following the rf burst was reduced to 1 μs by cutting off the receiver circuitry by application of a negative keying pulse during the action of rf field. Such an improvement is of particular importance for the observation of FID, since the latter immediately follows the end of the pulse due to strong inhomogeneous dephasing of the transverse nuclear magnetization in these samples.

In order to perform measurements in a dc pulsed magnetic field, a conventional video-pulse modulator output was applied to an accessory coil lightly coupled to the transmitter coil. Magnetic pulse strength at the center of this coil was estimated by taking into account the circuit current and its geometry and could be varied over the field range 0–5 Oe. By means of a variable delay line the occurrence of this dc field pulse could be varied over a wide range of times, making it possible to affect the nuclear spin system either during the rf pulses or after their removal.

In concluding this section we note that, regardless of the operating conditions, no shift in echo frequency with respect to the exciting pulse has ever been observed.

C. General experimental data

First, we note that the frequency dependence of the SPE and TPE amplitudes for a given sample are entirely consistent with each other. The shapes and widths of these spectra appreciably differ for different magnetic materials, providing the possibility of studying the behavior of the pulse responses under various excitation conditions. As an example, among the samples listed in Table I the broadest frequency spectrum with a half width σ of about 6×10^7 s^{-1} was observed on ^{55}Mn nuclei in NiMnSi, while the narrowest one with $\sigma = 9\times10^5$ s^{-1} was found to occur on ^{59}Co nuclei in Co_2MnSi. By addition of impurity or excess atoms in fcc Co, lithium ferrite or $Mn_{1-x}Sb_x$ all the NMR lines show a strong tendency to broaden, thereby considerably extending the range of frequencies where SPE can be observed. It should be noted also that the NMR spectra of several materials under investigation, such as Co-based alloys, hcp Co, $Mn_{1-x}Sb_x$, and some others, contain additional structure due to the magnetic hyperfine (hf) or quadrupole interactions. The center frequencies of the NMR lines ν_0 for the major group of magnets are presented in Table I.

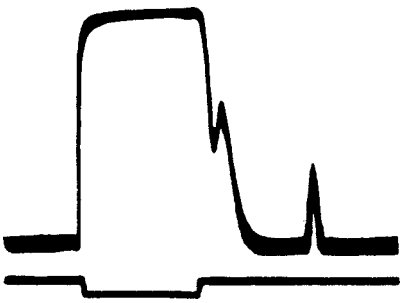

FIG. 1. Oscilloscope trace of the NMR signal of ^{59}Co in Co_2MnSi following a single exciting pulse of length $\tau_1 = 24\ \mu$s. Resonance frequency $\nu = \omega/2\pi = 145.2$ MHz temperature $T = 77$ K. An auxiliary beam along the bottom of the photograph is the signal from a video detector monitoring the rf pulse shape, amplitude and duration. The time scale is 10 μs/cm.

Figure 1 illustrates the typical trace of the temporal response of ^{59}Co nuclei in Co_2MnSi intermetallic compound to a single pulse of sufficient length ($\tau_1^{-1} \ll \sigma$) at the resonance frequency. This response can be actually considered as the result of a superposition of two coherent signals, that is, the FID that in the case examined lasts as long as the pulse itself, and the SPE appearing at the end of the FID. The initial transient of the FID envelope exhibits a characteristic peak due to the superemission effect.[22] The time occurrence of this original maximum is $t_m \sim \sigma^{-1}$ following the pulse.[22] Thus it is not obscured by the recovery time of the receiver for samples with relatively narrow NMR lines ($\sigma \lesssim 10^6$ s^{-1}) such as Co_2MnSi, lithium ferrite, and some others.

In contrast to the FID, for pulse lengths τ_1 of the order or shorter than the transverse relaxation time T_2 the SPE signals are readily detectable in all of the samples studied, for both domain and domain-wall nuclei, even though the excitation conditions are far from optimal. These signals show a simple, single-peaked structure whose width is approximately equal to that of the corresponding TPE responses. However, the ratio of the maximum SPE and TPE amplitudes I_m^S/I_m^T for a particular nuclear species does not generally exceed 10–15%. This ratio was found to be virtually independent of the particular material studied, the filling factor of the transmitter coil or the temperature of measurement

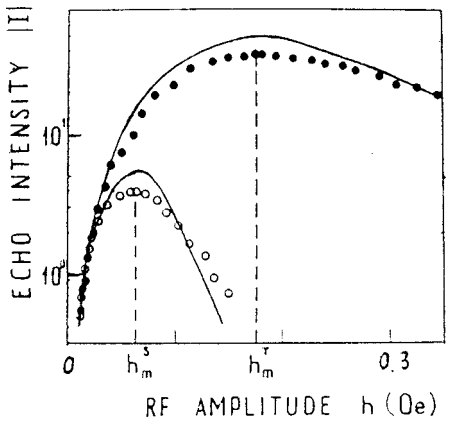

FIG. 2. Dependence of the single (○) and two-pulse (●) echo intensity (in arbitrary units) on the pulse amplitude h for the ^{55}Mn NMR in NiMnSb at $\nu=298.4$ MHz, $T=77$ K. The two-pulse case: $\tau_1=\tau_2=1.2\ \mu$s; the single-pulse case: $\tau_1=13\ \mu$s. Solid lines correspond to the calculated data for pulses of the same lengths and the following values of the other parameters: $\gamma^{Co}=6.36\times10^3$ Oe^{-1} s^{-1}, $\sigma=10^7$ s^{-1}, $\overline{\eta_0}=\Delta\eta_0=8\times10^2$, $\tau_l=\tau_t=1.5\ \mu$s, $\tau=10\ \mu$s, $\varphi_l=5/6\pi$, $\varphi_t=2/3\pi$. The calculated SPE intensity was matched to the experimental one by the appropriate choice of the $\tau_{l,t}$ and $\varphi_{l,t}$ values.

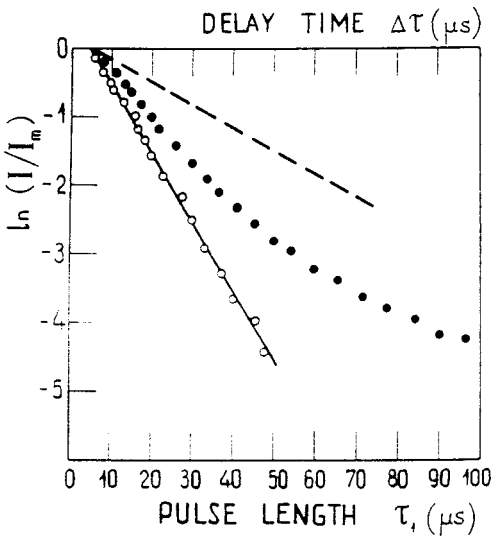

FIG. 3. Decays of the single (○) and two-pulse (●) echo intensities as a function of the pulse length τ_1 and the delay time between pulses $\Delta\tau$, respectively, for the NMR on ^{59}Co nuclei in pure fcc Co. Resonance frequency $\nu=217.2$ MHz; temperature $T=77$ K. The dashed line represents the SPE decay profile obtained by evaluating Eq. (10) for μ^+ of Eq. (4) with $\gamma^{Co}=6.36\times10^3$ Oe^{-1} s^{-1}, $h=0.1$ Oe, $\overline{\eta_0}=\Delta\eta_0=1.8\times10^3$, $\sigma=6\times10^6$ s^{-1}, $\tau_l=\tau_t=1\ \mu$s, $\varphi_l=\pi/2$, $\varphi_t=\frac{3}{4}\pi$. The solid line corresponds to the resultant decay of SPE intensity that was fitted to the experimental data by the appropriate choice of the pulse distortion parameters.

(at least within the temperature range used). It exhibited a tendency to decrease with increasing operating frequency, as may be seen from Table I.

In order to maximize the intensity of TPE, the amplitude of each of the two identical pulses h_m^T should be several times larger than the amplitude of the single pulse h_m^S required to produce the maximum of SPE. This fact is illustrated in Fig. 2, which shows the variation of the single and two-pulse echo intensities as a function of pulse amplitude in NiMnSb. Another feature to notice in Fig. 2 is that at low power levels the intensity of both signals increases as the third power of the pulse amplitude reaches a maximum at a certain value of $h_m^{S,T}$ and then monotonically decreases below the threshold for observation. The range of h values giving rise to the generation of SPE is much narrower than that of TPE.

Figure 3 represents the general trend of the TPE and SPE amplitudes as a function of the delay time between pulses $\Delta\tau$, and the pulse length τ_1, respectively, for the domain-wall resonance in pure fcc Co. These data indicate that the TPE transverse relaxation curve $I^T(\Delta\tau)$ is typically nonexponential, with a characteristic slowing down of the instantaneous decay rate for relatively long-time intervals between pulses ($\Delta\tau>40\ \mu$s). In contrast to the behavior of TPE, the SPE intensity varies approximately exponentially as $\exp[-2\tau_1/T_2^S]$ over the whole range of pulse lengths, except for the narrow initial region $\tau_1\lesssim4\ \mu$s in which a much sharper increase in the echo amplitude is experimentally observed (not shown in Fig. 3). On the other hand, for $\tau_1>5\ \mu$s the intensity of SPE decays generally more rapidly than the intensity of TPE. Consequently, a phenomenological time constant T_2^S determined from the SPE decay was estimated to be systematically smaller than the transverse relaxation time, T_2, defined from the initial slope of the TPE decay envelope. As follows from Table I, the relationship between these parameters for most of the samples is given by $T_2^S=(0.5-0.8)\ T_2$ in accordance with the earlier measurements.[12,14] Note that the above differences in the SPE and TPE decay kinetics have nothing to do with excitation of groups of nuclei located in different sections of the domain wall,[27] since all the measurements on a particular sample were performed at a fixed pulse amplitude corresponding to the largest intensity of SPE.

Finally, there is another phenomenon to be pointed out which actually lies beyond the scope of the present paper, but is of considerable interest for studying the relative properties of SPE and TPE signals. As well known,[28,29] in the presence of quadrupole interactions the TPE in magnets are expected to display a multiple structure due to the multiquantum transitions of nuclear spins in the nonequidistant system of energy levels. Such a structure of TPE including $2I$ single peaks separated by the time interval between pulses $\Delta\tau$ has been in fact observed by us in hcp Co in the frequency range 218.5–219.5 MHz, as well as in $Mn_{1-x}Sb_x$ within the concentration range $0.46\leqslant x\leqslant0.49$.[30] Without going into further detail we note here that similar structure in these samples was found to occur after a single-pulse excitation, so that the SPE signals are generated at times spaced by the pulse duration τ_1 and exhibit nearly the same behavior as the corresponding TPE responses.

D. Single- and two-pulse echoes in a dc pulsed magnetic field

From the previous section, it appears that the SPE and TPE behavior patterns are much the same. To explore the reasons for this similarity it is necessary to investigate the effect of pulse distortions on the SPE formation process. In

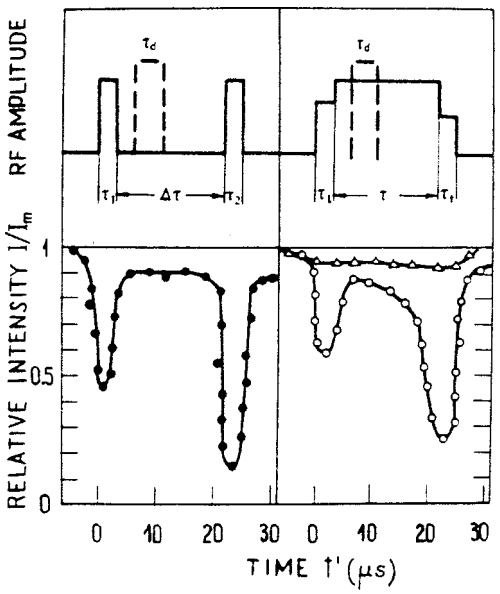

FIG. 4. Timing diagrams and intensity dependence of the two-pulse echo (●), single-pulse echo (○) and FID's original maximum (△) on the temporal location of a dc magnetic pulse of $H_d=5$ Oe lasting for a time interval τ_d along the corresponding time scales for the ^{57}Fe NMR in lithium ferrite. The data for two-pulse echo were taken with $\tau_1=\tau_2=0.8\ \mu$s, $\Delta\tau=21\ \mu$s, $\tau_d=3\ \mu$s, while the single-pulse echo data correspond to $\tau_1=25\ \mu$s, $\tau_d=5\ \mu$s. Resonance frequency $\nu=74.0$ MHz, $T=77$ K. The solid lines are drawn only to guide the eye.

the previous studies,[14] this has been done by means of an artificially-produced edge distortion of the exciting pulse. Such an approach, however, seems somewhat arbitrary, since the distortions obtained in this manner almost never occur under normal operating conditions.

To clarify the role of pulse distortions in the formation of SPE we made use of a quite different technique that suppresses the influence the rf pulse edges on the nuclear spin system. This was achieved by applying a dc magnetic field pulse of width τ_d and amplitude H_d whose timing could be varied so as to bring it into successive coincidence with either the leading or the trailing edges, as well as to keep it fixed within the central section or outside the rf pulse. Earlier,[31] this type of excitation has been used in a two-pulse echo sequence to estimate the static field required to shift a domain wall through a distance equal to its thickness d and to study anisotropic properties of the crystal.

Figure 4 represents the intensity dependence of TPE, SPE, and FID's original maximum in lithium ferrite on the dc magnetic pulse location. Similar plots hold for almost all samples under examination; however, the nonmonotonic behavior of the SPE and TPE amplitudes is best observed for relatively low driving fields ($\chi<\sigma$) when the major contribution to the echo height comes from nuclei at the center of the wall[27] (here $\chi=\gamma h\eta$ is the pulse amplitude in the sample expressed in the frequency units, γ the nuclear gyromagnetic ratio and η is the NMR enhancement factor in magnets).[32]

Let us consider in more detail the influence of the dc magnetic pulse on the intensity of TPE. As is well known,[33] the main effect of applying of external magnetic field to a multidomain ferromagnet is to shift the position of its domain walls, which in relatively small fields is of reversible character. If, therefore, the dc pulse H_d is superposed on one of the rf pulses it changes the location of the resonating nuclei within the domain wall (y direction) with respect to its center. This, in turn, is expected to decrease the nuclear enhancement factors which for 180° Bloch walls are known[34] to vary as $\eta=\eta_0\ \mathrm{sech}(y/d)$ where η_0 is the maximum enhancement at the center of the wall. Thus, if in the absence of the dc magnetic pulse the turning angles α_i of the two rf pulses $\alpha_{1,2}=\gamma h\eta\tau_{1,2}$ were chosen equal to each other in order to maximize the intensity of TPE,[35] after H_d is applied coincident with one of the exciting pulses the turning angles become significantly different. This drastically reduces the TPE amplitude.

An additional, more subtle effect takes place in systems with anisotropic hf interaction, due to the positional dependence of the nuclear resonance frequency within a domain wall.[36] This effect is responsible for the decrease in the TPE amplitude when H_d is applied between the two pulses or after the second pulse. It arises because the frequency shift partially destroys the phase coherence of the processing nuclear spins and reduces the overall efficiency of the rephasing process. Therefore, regardless of the temporal location of the dc magnetic pulse the TPE amplitude is expected to decrease; however, the change of the echo intensity is much larger when H_d completely overlaps one of the rf pulses.

The most striking feature of the data shown in Fig. 4 is that the behavior of single and two-pulse echoes in the pulsed magnetic field is virtually identical. The sharp decrease in the TPE intensity caused by superposition of the magnetic and one of the rf pulses is essentially similar to the reduction of SPE for H_d overlapping either of the edges of a long single pulse. Thus we conclude that the distorted edges of a sufficiently long pulse can be treated as a pair of individual pulses that explains the formation of SPE. As to the intensity of FID, it was found to exhibit no critical dependence upon the temporal location of H_d, as seen from Fig. 4.

The observed analogy in the SPE and TPE behavior patterns in the external magnetic field enable certain conclusions to be drawn concerning the distortion characteristics of the exciting rf pulse. In particular the essential point of our measurements is that the minimum length of a sufficiently strong magnetic pulse ($H_d>h$) which being superposed on one of the rf pulses leads to a noticeable reduction of the TPE intensity, is roughly 1.5 times greater than the rf pulse length itself. For comparison, a similar decrease in the SPE amplitude is observed only for magnetic pulse widths of about 1.5–1.8 μs. Thus it seems reasonable that the time duration of the edge distortions dominating the formation of SPE considerably exceed the rf pulse rise time, and for our present spectrometer are no shorter than 1.0 μs. In calculations of the SPE wave forms presented in Sec. III B below it will be shown that sufficiently long duration of the phase shifts at the edges of the pulse is one of the necessary conditions for the formation of SPE in the nuclear systems under consideration.

III. SINGLE-PULSE ECHO IN THE PULSE DISTORTION MODEL

A. General expressions

The transient response of the nuclear spin system to the action of various pulse sequences can be obtained from the

solution of Bloch's equations with a complete set of initial conditions giving the shapes of the pulses. Bloom, in his classic paper,[4] derived general expressions for the required response following any train of n exciting pulses having strictly rectangular shape ($n=1,2,3,...$). According to this paper, the transverse component of the nuclear magnetization, $\mu^+=\mu_x+i\mu_y$, after the application of a single pulse of resonant frequency ($\omega=\omega_0$) is given by

$$\mu^+/\mu_0=\frac{\chi}{\Phi}\left(\frac{2\delta}{\Phi}\sin^2\frac{\Phi\tau_1}{2}+i\ \sin\Phi\tau_1\right)\exp(-i\delta t), \quad (1)$$

whereas for two rectangular pulses of equal length $\tau_{1,2}$ and amplitude h near the echo formation time ($t=\Delta\tau$), it is of the form

$$\mu^+/\mu_0=\frac{\chi^3}{\Phi^3}\sin^2\frac{\Phi\tau_{1,2}}{2}\left(\frac{2\delta}{\Phi}\sin^2\frac{\Phi\tau_{1,2}}{2}-i\ \sin\Phi\tau_{1,2}\right)\exp[i\delta(\Delta\tau-t)]. \quad (2)$$

Here $\Phi=(\delta^2+\chi^2)^{1/2}$ is the angular frequency of precession of the magnetic moment about the effective field vector $\mathbf{H}_{\text{eff}}$ in the rotating frame of reference, $\delta=\omega_0-\omega_n$ the deviation of the Larmor frequency of a particular nucleus ω_n from the center frequency of the NMR line ω_0, μ_0 the equilibrium value of magnetization, and t the time following the last (the first for a FID and the second for a TPE) pulse. $\chi=\gamma h\eta$, as before, the rf pulse amplitude in frequency units multiplied by the enhancement factor.

Let us now consider the case when a single applied pulse contains phase distortions in the vicinity of its edges. Let us denote by φ and τ the phase and duration of the central steady-state section of the pulse, respectively, while φ_l and φ_t denote the phase shifts at its leading and trailing edges. The latter are assumed to remain constant during the lengths of the leading τ_l and trailing τ_t sections ($\tau_1=\tau_l+\tau+\tau_t$). The existence of the phase shifts at the edges of the pulse in the laboratory frame leads to the pulse's distortions in the rotating frame of reference that can be written as

$$h^+=h\begin{cases}\exp(i\varphi_l), & 0<t'<\tau_l,\\ \exp(i\varphi), & \tau_l<t'<\tau_l+\tau,\\ \exp(i\varphi_t), & \tau_l+\tau<t'<\tau_l+\tau+\tau_t,\end{cases} \quad (3)$$

where $h^+=h_x+ih_y$. The phase of the undistorted section of the pulse φ is taken equal to zero, with no loss of generality, and the time t' is measured from the beginning of the rf pulse.

By solving the Bloch equations[15] for the transverse component of the nuclear magnetization we obtain

$$\mu^+/\mu_0=[U_l(BB_t+DU_t+F^*F_t)+U_l^*(FB_l+B^*F_t+D^*U_t)+R_l(UB_t+RU_t+U^*F_t)]\exp(i\delta t), \quad (4)$$

where

$$U=\frac{\chi}{\Phi}\left(-\frac{2\delta}{\Phi}\sin^2\frac{\Phi\tau}{2}+i\ \sin\Phi\tau\right)\exp(i\varphi),$$

$$B=\cos\Phi\tau+\left(\frac{\chi}{\Phi}\right)^2\sin^2\frac{\Phi\tau}{2}+i\ \frac{\delta}{\Phi}\sin\Phi\tau,$$

$$R=1-2\left(\frac{\chi}{\Phi}\right)^2\sin^2\frac{\Phi\tau}{2},$$

$$F=\left(\frac{\chi}{\Phi}\right)^2\sin^2\frac{\Phi\tau}{2}\exp(2i\varphi),$$

$$D=\frac{U}{2}\exp(-2i\varphi). \quad (5)$$

The coefficients with the subscripts in Eq. (4) can be readily obtained by replacing τ by $\tau_{l,t}$ and φ by $\varphi_{l,t}$, while the time t is measured, as usual, from the trailing edge of the applied pulse, i.e., $t=t'-(\tau_l+\tau+\tau_t)>0$.

Equations (1), (2), and (4) describe the contribution of a single spin packet to the intensity of the corresponding signals. In order to evaluate the shapes of these signals in nonmagnetic or weakly magnetic substances ($\eta\approx1$) the magnetization of individual spin packets has to be integrated over the inhomogeneous line-shape function $g(\delta)$ thus yielding

$$I(h,t)=\left|\int_{-\infty}^{+\infty}\mu^+(\delta,h,t)g(\delta)d\delta\right|, \quad (6)$$

where $g(\delta)$ can be assumed to be a symmetrically shaped Gaussian distribution, of the form

$$g(\delta)=\left[\frac{\ln 2}{\pi}\right]^{1/2}\sigma^{-1}\exp[-\ln 2(\delta/\sigma)^2]. \quad (7)$$

For magnetic materials, the NMR signals are generated in strong internal hf fields produced at nuclei by the electron spin system of the crystal. This naturally results in enhancement of the rf field being most pronounced for the domain-wall nuclei. For this reason, in most cases the zero-field NMR signals originate predominantly in the latter regions of a multidomain ferromagnet.[24] However, in the special cases discussed in Sec. II A, the major contribution to the echo intensity is associated with the domain nuclei.

Another prominent feature of pulsed NMR in magnets is the essentially inhomogeneous distribution of enhancement factors η over the volume of the sample. This can be explicitly incorporated into the analysis by means of the enhancement factor distribution function $F(\eta)$, which, according to Ref. 25, differs appreciably for the domain and domain-wall resonance. In particular, for domain nuclei this function can be represented as

$$F_D(\eta)=\left(\frac{\ln 2}{\pi}\right)^{1/2}\Delta\eta^{-1}\exp\left(-\ln 2\frac{(\eta-\overline{\eta})^2}{\Delta\eta^2}\right), \quad (8)$$

while for the nuclei located in 180° Bloch walls to within a multiplying constant it is defined by the expression

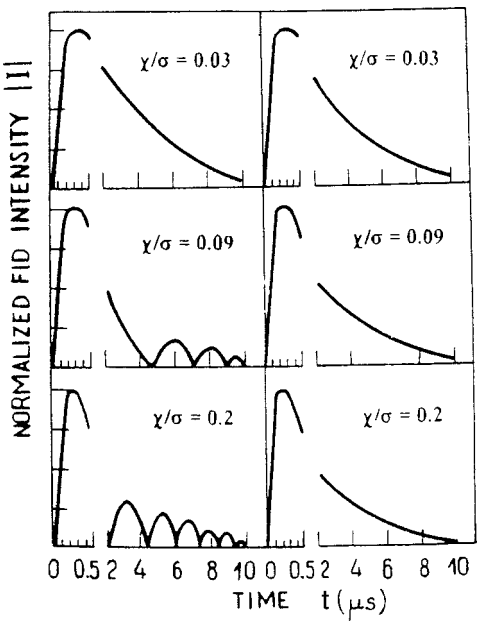

FIG. 5. Computer plots of the FID amplitude as a function of time for various constant χ/σ values obtained in the model of rectangular pulses. The left-hand column: the numerical integration of Eq. (6) for μ^+ of Eq. (1) for a unique rf spin excitation in nonmagnetic materials ($\eta=1$); the right-hand column: the numerical integration of Eq. (10) for $F(\eta)$ of Eq. (8) for the domain resonance in magnets. Parameters used in the calculations are $\sigma=10^7\ \mathrm{s}^{-1}$, $\tau_1=10\ \mu\mathrm{s}$, $\overline{\eta}=\Delta\eta=100$. The initial section of time axis is expanded by a factor of 5 to show the exact timing of the FID's original maximum.

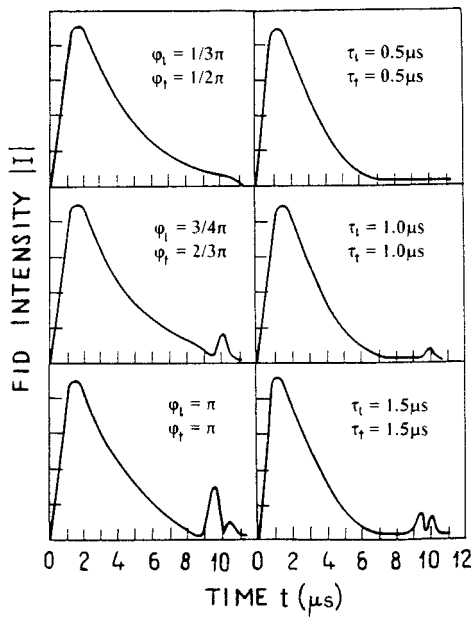

FIG. 6. Temporal response of the nuclear spin system following a phase-shift pulse obtained by the numerical evaluation of Eq. (10) for μ^+ of Eq. (4) and $F(\eta)$ of Eq. (9) as a function of edge distortion parameters. The left-hand column: $\tau_l=\tau_t=1\ \mu\mathrm{s}$, $\gamma h=3\times10^3\ \mathrm{s}^{-1}$; the right-hand column: $\varphi_l=\frac{7}{12}\pi$, $\varphi_t=\frac{5}{6}\pi$, $\gamma h=10^4\ \mathrm{s}^{-1}$. The other parameters used in the calculations are $\sigma=10^6\ \mathrm{s}^{-1}$, $\overline{\eta_0}=\Delta\eta_0=100$, $\tau=10\ \mu\mathrm{s}$.

$$F_W(\eta)=\eta^{-1}\int_0^{\infty}\exp\left(-\ln 2\,\frac{[(\varepsilon^2+\eta^2)^{1/2}-\overline{\eta_0}]^2}{\Delta\eta_0^2}\right)d\varepsilon. \tag{9}$$

Here $\overline{\eta}$ is the average value of the domain enhancement factor, $\overline{\eta_0}$ the maximum enhancement at the center of the wall averaged over all domain walls of the sample, $\Delta\eta$ and $\Delta\eta_0$ the widths of the corresponding distribution functions, and $\epsilon=(\eta_0^2-\eta^2)^{1/2}$.

Therefore, the final expression for the pulsed NMR responses from any magnetic substance at arbitrary temperature may be given as

$$I(h,t)=\left|\int_0^{\infty}\eta F_{D,W}(\eta)d\eta\int_{-\infty}^{+\infty}\mu^+(\eta,\delta,h,t)g(\delta)d\delta\right|. \tag{10}$$

In writing down the above equations we have ignored the frequency dependence of the enhancement factors, which is valid for the case of uniform wall rotation,[36] and have neglected the effect of relaxation processes on the NMR signal intensity.

B. Numerical results

The starting point of our calculations was to evaluate numerically the shape of the pulse responses involved in the model of rectangular pulses. The results of such calculations obtained for nonmagnetic materials for a sufficiently long square pulse ($\tau_1^{-1}<\sigma$), are plotted in Fig. 5. The data indicate that for relatively small pulse areas $\alpha_1=\gamma h\tau_1<2\pi$ the FID is a smoothly varying function of time. For $\alpha_1\gtrsim2\pi$, however, it displays a continuous train of oscillations, the main characteristics of which are essentially the same as calculated previously for atomic or spin two-level systems.[22,23]

At the same time the inclusion of inhomogeneity of enhancement factors ($\Delta\eta/\overline{\eta}\gtrsim0.03$) into the calculations, which typically occurs even for monodomain particles,[33] smears out completely the oscillations in the FID curve. Thus immediately following the end of the pulse, the FID signal rises rapidly from zero for $t=0$, reaches an original maximum at $t_m=\sigma^{-1}\ln(\sigma/\chi)$,[22] and then decreases monotonically in amplitude before vanishing precisely at $t=\tau_1$, as shown in Fig. 5. Similar FID behavior can be obtained by the numerical integration of Eq. (10) for $F(\eta)$ given by Eq. (9) corresponding to the domain-wall resonance.

The results of the calculations show satisfactory agreement with the experimentally observed FID shapes, both for the domain and domain-wall nuclei [see Sec. II C]. However, they conclusively indicate that exactly rectangular pulses are essentially unable to produce the SPE. Accordingly, further calculations were performed in the pulse distortion model, in which the edge distortion characteristics were assumed to be virtually independent of the duration and amplitude of the steady-state section of the pulse. Figure 6 demonstrates the development of the signal profiles produced by a single phase-shift pulse that are of interest for interpreting experimentally observed SPE patterns. The existence of these distortions does not change appreciably the FID shapes in the time interval $0<t<\tau_1$. However, for a long pulse excitation ($\tau_1^{-1}<\sigma$) at $t\approx\tau_1$, they create an additional maximum that exhibits all the usual characteristics of SPE.

The possibility of formation of SPE, and the resultant SPE wave forms and amplitudes, are strongly dependent upon the phase shifts and duration of the edge distortions. In particular, sufficiently long duration of the phase shifts ($\tau_{l,t}^{-1}<\sigma$) was found to be one of the fundamental conditions for the formation of SPE.[37] For shorter $\tau_{l,t}$, the $I(t)$ curve at $t=\tau_1$ exhibits no SPE; however, as $\tau_{l,t}$ is increased a range of values is found to give rise to the formation of SPE. The intensity of the latter gradually increases, while its structure is transformed from the single- to the double-peaked one with the double peaks separated approximately by the duration $\tau_{l,t}$ of the edge distortions [see Fig. 6].

On the other hand, for the phase shifts $\varphi_{l,t}<\pi/2$ no echoes could be obtained for all reasonable values of $\tau_{l,t}$ used in our calculations. In order to produce a SPE the $\varphi_{l,t}$ phase shifts should be equal to or exceed $\pi/2$. However, the SPE may appear also in the case when this requirement is satisfied at least at one of the edges. For example, if the phase shift near the trailing edge of the pulse φ_t is close to π the SPE of an asymmetric double-peaked shape is readily seen over the whole range of φ_l values including $\varphi_l=0$ (no distortion at the leading edge). This strongly confirms the idea of the major role of the trailing edge in the formation of SPE, and is consistent with our experiments in the dc pulsed magnetic field, as illustrated in Fig. 4.

So far we have considered general features of SPE, as functions of the edge distortion parameters. In the following, we concentrate on the SPE intensity dependence upon the width and amplitude of the undistorted section of the pulse, assuming that the edge distortion characteristics ensure the generation of the single-peaked SPE.

One of the most interesting results of the computation is the monotonic increase of the SPE intensity with decreasing pulse length τ, as seen in Fig. 3. At the first sight this behavior might seem somewhat unexpected, since the numerical analysis presented here has completely neglected relaxation effects. However, as will be discussed in Sec. IV, it arises quite naturally for reasons intrinsic to the formation of SPE within the pulse distortion model. In this approximation, for sufficiently long τ_1 (precluding superposition of the SPE and FID signals) the $I^S(\tau_1)$ dependence is strictly exponential with the time constant T_2^P, which is mainly determined by the pulse distortion characteristics.

As was outlined in Sec. II C, the SPE decay time T_2^S for most of the samples was found to be 1.25 to 2.0 times smaller than the transverse relaxation time T_2 deduced from the corresponding TPE dependence $I^T(\Delta\tau)$. This fact can be attributed to the existence of a specific mechanism contributing to the SPE intensity decay, in addition to the normal transverse relaxation mechanism. As usual, assuming no correlation between the latter processes and those relevant only to the SPE formation mechanism, the resultant decay of the SPE intensity can be represented as the product of the two exponents with the single relaxation rate

$$(T_2^S)^{-1}=T_2^{-1}+(T_2^P)^{-1}. \tag{11}$$

The SPE thus decays at a rate determined by both transverse relaxation and pulse distortion effects.

It turns out that in most cases the phase shifts at the edges of the pulse and thus the numerical values of T_2^P can be chosen such that the calculated SPE intensity decay will reproduce adequately the corresponding experimental behavior. The fits obtained for pure fcc Co are displayed in Fig. 3. Here, the dashed line shows the calculated dependence of the SPE amplitude on the pulse width for $\varphi_l=\pi/2$ and $\varphi_t=\frac{3}{4}\pi$ which yields a value $T_2^P=60\ \mu$s, while the solid line gives the overall echo decay kinetics with the time constant $T_2^S=20\ \mu$s, obtained from Eq. (11) for $T_2=30\ \mu$s (T_2 was independently measured via TPE).

Apart from the pulse duration, the SPE intensity is strongly affected by the pulse amplitude h. The typical plot of the SPE height as a function of applied rf field calculated for NiMnSb is presented in Fig. 2. Similar calculations performed for a wide range of parameters clearly indicate that the general shape of $I^S(h)$ curve and the position of its maximum are essentially independent of the phase $\varphi_{l,t}$ and duration $\tau_{l,t}$ of the edge distortions. This justifies the representation in the same Fig. 2 of both the single- and two-pulse echo $I(h)$ curves, although the latter has been obtained by the numerical integration of Eqs. (10) and (2) in the model of rectangular pulses.

On the other hand, according to our analysis, the position of the $I^S(h)$ maximum is determined exclusively by the parameters characterizing the undistorted section of the pulse, that is, τ and h. In particular, the optimum turning angles of this section that yield the largest SPE amplitude are equal to

$$\alpha^m=\gamma h_m^S\overline{\eta_0}\tau=(1.00\pm0.05)\pi. \tag{12}$$

This implies that the decrease of one of the parameters in the expression for α^m leads to the proportional increase of the other so that the optimum turning angles remain essentially constant. For example, as $\overline{\eta_0}$ is reduced, τ being fixed, the maximum of the SPE intensity shifts towards higher values of h_m^S. Similar shifts in the echo peak are observed by varying the pulse length τ for any given values of γ and $\overline{\eta_0}$.

Thus the position of the maximum in the $I^S(h)$ experimental curve provides definite information on the average value of enhancement factor at the center of the walls $\overline{\eta_0}$. By analogy, similar information can be obtained also by studying the TPE intensity dependence on the rf amplitude.[34,35] The values of $\overline{\eta_0}$ estimated using both the single- and two-pulse echo techniques were found to coincide with each other to within experimental error, as seen from the last column of Table I.

To close this section, we note that the substitution of Eq. (8) for Eq. (9) when evaluating Eq. (10) produces no significant effect on the time dependence of the calculated SPE wave forms. This indicates that the main characteristics of SPE reported in this section apply also to the signal originating from the domain nuclei in agreement with our measurements on thin ferromagnetic films. However, the dependence the SPE amplitude upon h, $I^S(h)$, is roughly affected by the explicit form of $F(\eta)$ function used in the calculations, making it possible to identify the domain or the domain-wall origin of the NMR signals just as in the case of TPE.[25]

IV. DISCUSSION AND CONCLUSIONS

The results of the present paper unambiguously indicate that the dephasing of the nuclear spins after the application

of a single undistorted pulse is irreversible, i.e., a square rf exciting pulse fails to produce SPE. In order to generate SPE the direction of the effective magnetic field $\mathbf{H}_{\text{eff}}$ in the rotating frame of reference must change during the action of rf pulse. This condition is satisfied for a pulse with distorted edges, which necessarily arise in the course of its generation, due to the nonideal properties of the electronic circuitry's components.

In analyzing the formation of SPE in the model of phase-shift pulses we assume that the effect of the pulse edges upon the sample is close to that of two individual pulses. From this point of view, the SPE formation process closely resembles that of the TPE, which in the nuclear systems under consideration occurs through the phase rephasing mechanism.[2] According to this mechanism, the leading edge of the pulse flips the macroscopic magnetisation away from the initial z direction. Then during the stable section of the pulse the transverse magnetization acquires an inhomogeneous phase. Next, the trailing edge causes a cumulative phase reversal, and finally the inhomogeneous phase advance is compensated near the time $t=\tau_1$. In this approach the most significant conditions required for the formation of SPE can be summarized as follows: (i) the phase of the distorted edges must differ significantly from the steady-state section of the pulse, (ii) the lengths of the phase shifts must be long enough to provide sufficiently large angles of rotation $\alpha_{l,t}=\gamma h\overline{\eta_0}\tau_{l,t}$ which, according to our calculations, should be no smaller than 0.3 rad, (iii) the time duration of the stationary section of the pulse must be greater than the inverse NMR line half width, but smaller than T_2: $\sigma^{-1}<\tau<T_2$.

To discuss these conditions in more detail we note first that the calculated SPE wave forms are sensitive functions of the pulse distortion parameters, which are themselves governed by the arrangement and interconnection of the electronics employed. This is believed to account for previous experimental observations, according to which the SPE may assume either a double-[9] or a single-peaked structure[11,14] or may be not detectable at all.[38]

The single-peaked profile of SPE in all the samples studied suggests that the phase shifts at the edges of pulses generated by our present apparatus cover the range $2/3\pi\lesssim\varphi_{l,t}\lesssim 5/6\pi$, while their duration, $\tau_{l,t}$, is approximately of 1.0–1.5 μs. This situation apparently holds for most of the pulsed NMR spectrometers operating in the meter band, since the majority of investigations[11–14,16] show a single-peaked structure for the SPE. The decrease in the relative SPE intensity with increasing the excitation frequency, clearly seen from Table I and supported by measurements on a range of other alloys and compounds mentioned in Sec. II A, can be attributed to the frequency dependence of the pulse distortion parameters. However, this dependence does not seem sufficiently strong to suppress the production of SPE or to transform its shape.

The similarity in the single- and two-pulse echo formation mechanisms is likely to account for the similar behavior of the corresponding responses. In fact, as was outlined in Secs. II C and III B, this similarity manifests itself in essentially identical information, which can be obtained by studying the intensity of these signals as a function of the pulse frequency and amplitude, the natural occurrence of multiple single and two-pulse echoes in quadrupolar split systems, the dependence of the echo envelopes on the pulse turning angles, and so on.

However, the principal difference between the SPE and TPE formation mechanisms is that between the edges of a single applied pulse there exists a rf field of resonance frequency which is absent for a two-pulse excitation. The effect of this field is twofold. Firstly, it generates the FID, and, secondly, it selects the nuclear spins that contribute significantly to the SPE.

For magnetic materials one has to allow for a spread in values of enhancement factors. This implies that during the steady-state section of the pulse the nuclear spins become randomly distributed over both the turning angles α and the frequency detunings δ so that the process of their rephasing by the trailing edge of the pulse cannot be uniformly effective. In particular, the nuclear spins having large angles of rotation $\alpha\gg\pi$ and equal but opposite sign detunings $\delta=\pm\chi$ are known to generate the FID,[33,39] while the existence of edge distortions does not noticeably affect the process of their dephasing. At the same time, as discussed in Sec. III B, the nuclear moments rotated through relatively small turning angles $\alpha\approx\pi$ by the central section of the pulse, after the action of its trailing edge, generally produce the SPE.

The above argument can be used to account for the observed differences in the SPE and TPE behavior patterns illustrated in Figs. 2 and 3. If, after a two-pulse sequence, all spins excited by the pulses take part in the formation of TPE, then after the action of a single pulse only a small fraction of resonance spins, for which during the central section of the pulse Eq. (12) is satisfied, contribute explicitly to the SPE intensity. For this reason, as well as the relatively small angles of rotation caused by the distorted edges, the SPE amplitude is generally much smaller than that of the TPE. Further, the pulse lengths in the two-pulse technique are commonly much shorter than the duration of the single pulse producing SPE; thus to achieve the optimum turning angles $\alpha^m_{1,2}=\gamma h^T_m\overline{\eta_0}\tau_{1,2}=1.2$ rad required to maximize the TPE the pulse amplitudes must be correspondly larger than in the case of SPE. Finally, with increasing rf amplitude in the region $h>h^s_m$ the number of spins having α^m angles compatible with Eq. (12) rapidly decreases, resulting in a relatively narrow range of h values giving rise to the formation of SPE [see Fig. 2].

A similar interpretation may be given for the observed distinctions in the single- and two-pulse echo decay kinetics presented in Fig. 3. First, we note that the large departure of the TPE intensity from exponential decay, which arises from inhomogeneity of the transverse relaxation time T_2 across the domain walls[27,40] is most apparent for large values of $\Delta\tau$. Because of the relatively small intensity of SPE the $I^S(\tau_1)$ measurements for the samples under investigation may be performed only in a limited range of pulse lengths $\tau_1<30-40$ μs, over which the SPE amplitude decays nearly exponentially, just as in the case of TPE. At the same time, as was pointed out in Sec. III B, the acceleration of the SPE decay with respect to the TPE may be related to the specific mechanism of SPE formation that contributes to the observed reduction in the SPE intensity in conjunction with pure relaxation processes. Indeed, in terms of the pulse distortion model the rise in the SPE amplitude with decreasing pulse duration in the absence of transverse relaxation can be

attributed to an increase of the total number of spins that satisfy Eq. (12) and thus contribute strongly to the intensity of SPE. On the other hand, for very short pulses this additional pseudorelaxation process is expected to become ineffective, because of the absence of the necessary dephasing of the nuclear spins during the applied pulse. Hence one might think that the $I^S(\tau_1)$ curve would be likely to exhibit a characteristic maximum at a certain τ_1 value, which for our samples was estimated to vary within the range 1.5–4.0 μs.

Experimentally, for all of the samples studied here, decreasing τ_1 causes the SPE amplitude to increase monotonically before becoming indistinguishable in the FID. The most probable reason for such a behavior is that under certain experimental conditions, especially for narrow NMR lines being excited by relatively short pulses, the FID duration may greatly exceed the pulse duration, leading to a superposition of the FID and SPE amplitudes.[12,14] Therefore, in the range $\tau_1^{-1} > \sigma$ the intensity of SPE gradually increases without any noticeable tendency to saturation.

In conclusion, we note that the model developed in this paper can be successfully applied to analyze several other related NMR pulse-echo phenomena, in particular, the two-pulse stimulated echo generated by two long pulses of different lengths, τ_1 and τ_2, at times $t = \tau_1 - \tau_2$ and $t = \tau_1$ after the termination of the second pulse.[11,17] These responses cannot be obtained from a pair of exactly rectangular pulses, since in the absence of relaxation effects the FID of the second pulse is just that given by Eq. (1) (Ref. 4) and, as a consequence, for $t > t_m$ it displays only a monotonic decrease in the signal intensity [see the right-hand column in Fig. 5]. On the other hand, this phenomenon can be interpreted quite naturally in terms of the pulse distortion model, since the stimulated echoes in this case are in fact produced by three exciting pulses, two of which are created by the edges of the first pulse, while the third is generated by either the leading or the trailing edge of the second pulse. A similar approach may be used to explain multiple two-pulse echoes arising after the application of two long pulses of unequal lengths.[41] However, a more detailed analysis of these phenomena is beyond the scope of our present discussion. Finally, there is reason to believe that the developed approach may be, in principle, extended to pulse excitations in different physical systems. The main point of our argument is that pulse distortions of various types are known to arise over a wide range of radio, optical, and acoustical frequencies.[8,19,42]

ACKNOWLEDGMENTS

The authors wish to thank L. L. Buishvili and L. M. Folan for helpful discussions and T. I. Kvaratskhelia for assistance with the computation.

[1] F. Bloch, Phys. Rev. **70**, 460 (1946).
[2] E. L. Hahn, Phys. Rev. **80**, 580 (1950).
[3] R. W. Gould, Phys. Rev. Lett. **19**, 477 (1965).
[4] A. L. Bloom, Phys. Rev. **98**, 1105 (1955).
[5] R. J. Blume, Phys. Rev. **109**, 1867 (1958).
[6] A. Szabo and M. Crall, Opt. Lett. **1**, 10 (1978).
[7] B. P. Smolyakov and E. P. Khaimovich, Zh. Eksp. Teor. Fiz. **76**, 1303 (1979) [Sov. Phys. JETP **49**, 661 (1979)].
[8] K. Fossheim, K. Kajimura, T. G. Kazyaka, R. L. Melcher, and N. S. Shiren, Phys. Rev. B **17**, 964 (1977).
[9] M. B. Stearns, AIP Conf. Proc. **10**, 1644 (1973).
[10] Yu. Bunkov, B. S. Dumesh, and M. I. Kurkin, Pis'ma Zh. Eksp. Teor. Fiz. **19**, 216 (1974) [JETP Lett. **19**, 132 (1974)].
[11] D. K. Fowler, D. C. Creagh, R. W. N. Kinnear, and G. V. H. Wilson, Phys. Status Solidi A **92**, 535 (1985).
[12] V. P. Chekmaryov, M. I. Kurkin, and S. I. Goloshchapov, Zh. Eksp. Teor. Fiz. **76**, 1675 (1979) [Sov. Phys. JETP **49**, 851 (1979)].
[13] V. P. Chekmaryov and G. I. Mamniashvili, Fiz. Met. Metalloved. **51**, 685 (1981).
[14] V. I. Tsifrinovich, E. S. Mushailov, N. V. Baksheyev, A. M. Bessmertny, E. A. Glozman, V. K. Maltsev, O. V. Novosyolov, and A. E. Reingardt, Zh. Eksp. Teor. Fiz. **88**, 1481 (1985) [Sov. Phys. JETP **61**, 886 (1985)].
[15] V. I. Tsifrinovich, *Echo Signals Calculation* (Nauka, Novosibirsk, 1986) (in Russian).
[16] D. K. Fowler, D. H. Chaplin, and G. V. H. Wilson, J. Magn. Reson. **66**, 369 (1986).
[17] I. G. Kiliptari, Fiz. Tverd. Tela **34**, 1418 (1992) [Sov. Phys. Solid State **34**, 753 (1992)].
[18] S. Mason and H. Zimmerman, *Electronic Circuits, Signals, and Systems* (Wiley, New York, 1960).
[19] E. M. Verestchagin, *Modulation in Superhigh Frequency Generators* (Sov. Radio, Moscow, 1972) (in Russian).
[20] U. Haeberlen, *High Resolution NMR Studies in Solids* (Academic, New York, 1976).
[21] J. S. Waugh, *New NMR Methods in Solid State Physics* (Mir, Moscow, 1978) (in Russian).
[22] A. Schenzle, N. C. Wong, and R. G. Brewer, Phys. Rev. A **21**, 887 (1980).
[23] M. Kunitomo, T. Endo, S. Nakanishi, and T. Hashi, Phys. Rev. A **25**, 2235 (1982).
[24] C. H. Cobb, V. Jaccarino, and M. A. Butler, Phys. Rev. B **7**, 307 (1973).
[25] I. G. Kiliptari, Phys. Rev. B **52**, 7346 (1995).
[26] G. D. Webber and P. C. Riedi, J. Phys. F **14**, 1159 (1981).
[27] R. L. Streever, Phys. Rev. **134A**, 1612 (1964).
[28] H. Abe, H. Yasuoka, and A. Hirai, J. Phys. Soc. Jpn. **21**, 77 (1966).
[29] V. I. Tsifrinovich, Zh. Eksp. Teor. Fiz. **94**, 208 (1988) [Sov. Phys. JETP **68**, 1413 (1988)].
[30] T. Sh. Abesadze, A. M. Akhalkatsi, I. G. Kiliptari, M. G. Melikiya, and T. M. Shavishvili, Zh. Eksp. Teor. Fiz. **96**, 187 (1989).
[31] R. H. Dean and R. J. Urwin, J. Phys. C **3**, 1747 (1970).
[32] E. A. Turov and M. P. Petrov, *Nuclear Magnetic Resonance in Ferro- and Antiferro-magnets* (Wiley, New York, 1972).
[33] M. I. Kurkin and E. A. Turov, *NMR in Magnetically Ordered Substances: Theory and Applications* (Nauka, Moscow, 1990) (in Russian).
[34] M. B. Stearns, Phys. Rev. **162**, 496 (1967).
[35] I. G. Kiliptari and M. I. Kurkin, Fiz. Met. Metalloved. **8**, 81

(1992) [Phys. Met. Metallogr. **74**, 136 (1992)].
[36] H. P. Kunkel and C. W. Searle, Phys. Rev. B **23**, 65 (1981).
[37] For magnetic materials having broad frequency spectra, the σ parameter should be replaced by the half of the total bandwidth of the receiver circuit, since the latter cuts off the range of frequencies contributing to the NMR signals.
[38] D. K. Fowler, D. C. Creagh, and G. V. H. Wilson, Phys. Status Solidi A **94**, K97 (1986).
[39] W. B. Mims, Phys. Rev. **141**, 499 (1966).
[40] I. G. Kiliptari, Fiz. Tverd. Tela **35**, 1232 (1993) [Sov. Phys. Solid State **35**, 627 (1993)].
[41] A. E. Reingardt, V. I. Tsifrinovich, O. V. Novosyolov, and V. K. Maltsev, Fiz. Tverd. Tela **25**, 3163 (1983) [Sov. Phys. Solid State **25**, 1823 (1983)].
[42] L. Armstrong and S. Feneuille, in *Multiphoton Processes* (Wiley, New York, 1977), p. 237.